sCIP-ing towards streamlined chemoproteomics

Nikolas R. Burton[‡†] and Keriann M. Backus[‡†§‖⊥#*]

† Department of Biological Chemistry, David Geffen School of Medicine, UCLA, Los Angeles, California 90095, United States

‡ Department of Chemistry and Biochemistry, UCLA, Los Angeles, California 90095, United States

§ Molecular Biology Institute, UCLA, Los Angeles, California 90095, United States

‖ DOE Institute for Genomics and Proteomics, UCLA, Los Angeles, California 90095, United States

⊥ Eli and Edythe Broad Center of Regenerative Medicine and Stem Cell Research, UCLA, Los Angeles, California 90095, United States

Jonsson Comprehensive Cancer Center, UCLA, Los Angeles, California 90095, United States

* Corresponding Author: Keriann M. Backus, Biological Chemistry Department, David Geffen School of Medicine, UCLA, Los Angeles, CA, 90095, USA, E-mail: kbackus@mednet.ucla.edu

ABSTRACT

Mapping the ligandability or potential druggability of all proteins in the human proteome is a central goal of mass spectrometry-based chemoproteomics. Achieving this ambitious objective requires high throughput and high coverage sample preparation and LC-MS/MS analysis for hundreds to thousands of reactive compounds and chemical probes. Conducting chemoproteomic screens at this scale benefits from technical innovations that achieve increased sample throughput. Multiplexed analysis using commercially available amine-reactive isobaric reagents (e.g. tandem

https://doi.org/10.26434/chemrxiv-2023-0szhj **ORCID:** https://orcid.org/0000-0001-8541-1404 Content not peer-reviewed by ChemRxiv. **License:** CC BY-NC-ND 4.0

mass tags or TMT) is a favored strategy to decrease instrument acquisition time. These reagents are ideally suited for protein-based quantification applications, with efficient capping and pooling of peptides after sequence specific digestion. The added enrichment steps in nearly all chemoproteomic sample preparation workflows reveals a still largely untapped opportunity for isobaric labeling, namely incorporation of the TMT label into the chemoproteomic enrichment handle for early sample pooling and increased sample preparation throughput. Here we realize this vision by establishing the silane-based Cleavable Linkers for Isotopically-labeled Proteomics (sCIP)-TMT proteomic platform. sCIP-TMT pairs a custom click-compatible sCIP capture reagent that is readily functionalized in high yield with commercially available TMT tags. Synthesis and benchmarking of a 10-plex set of sCIP-TMT reveals a 1.5-fold decrease in sample preparation time together with high coverage and high accuracy quantification. By screening a focused library of cysteine-reactive electrophiles, we demonstrate the utility of sCIP-TMT for chemoproteomic target hunting, identifying 789 total liganded cysteines. Distinguished by its compatibility with established enrichment and quantification protocols, we expect sCIP-TMT will readily translate to a wide range of chemoproteomic applications.

https://doi.org/10.26434/chemrxiv-2023-0szhj **ORCID:** https://orcid.org/0000-0001-8541-1404 Content not peer-reviewed by ChemRxiv. **License:** CC BY-NC-ND 4.0

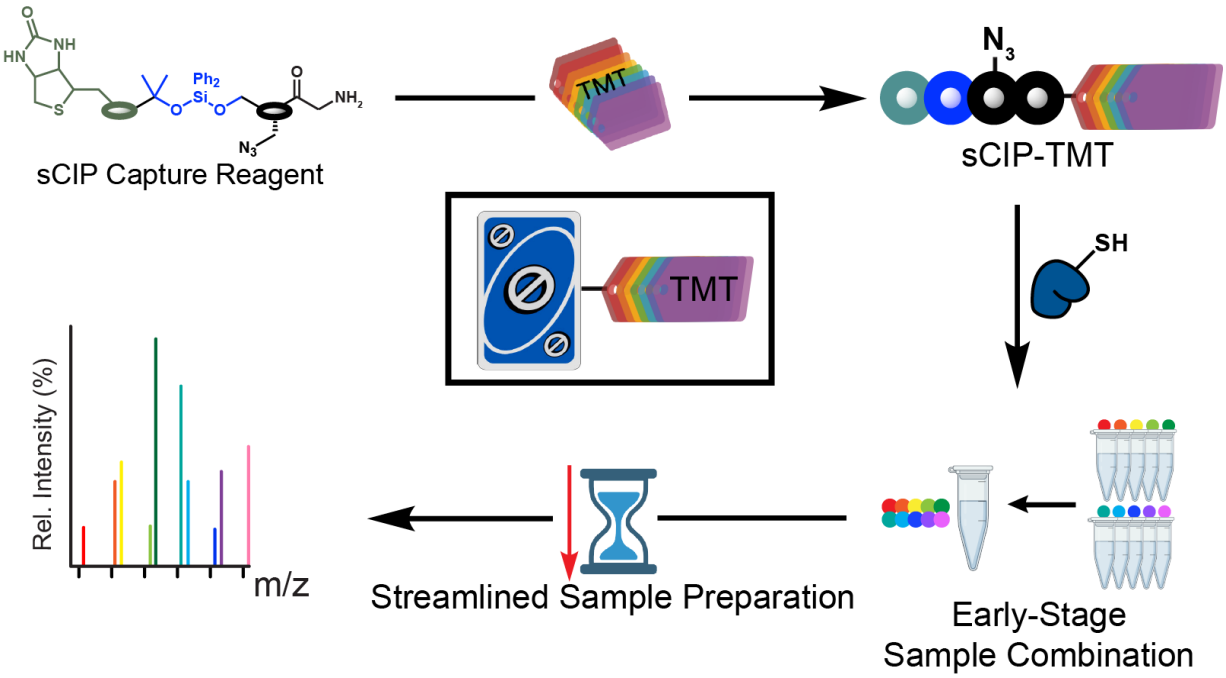

INTRODUCTION

Mass spectrometry-based quantitative chemoproteomics is an enabling technology for functional biology and drug discovery. Showcasing the widespread impact of chemoproteomics, recent studies have uncovered covalent degraders[1–6], novel targets with anti-bacterial activity[7,8], pinpointed redox sensitive cysteines[9–14], mapped small-molecule-protein binding sites[15–22], and discovered latent electrophiles[23,24]. A key objective of established chemoproteomics platforms is the proteome-wide identification of the protein targets and specific residues modified by covalent chemical probes, which can serve as launchpoint for drug development campaigns. Towards this objective, many research groups focus on technical innovations in three key areas: (1) covalent labeling chemistries, (2) improved sample preparation workflows that improve coverage and reduce sample loss, (3) decreased instrument acquisition time through improved instrumentation and sample multiplexing.

Substantial advances have been made in the development of covalent labeling chemistries. Chemoproteomics platforms are now available that analyze reversible binders[21,22,25] and map all nucleophilic amino-acid side chains[26], including serine[27–29], lysine[17,30–32],

https://doi.org/10.26434/chemrxiv-2023-0szhj **ORCID:** https://orcid.org/0000-0001-8541-1404 Content not peer-reviewed by ChemRxiv. **License:** CC BY-NC-ND 4.0

tyrosine[31,33,34], methionine[35,36], aspartate and glutamate[37–39], arginine[40], and cysteine[9,16,41,42]. While these exciting advances in chemical probe technology have improved our understanding of the landscape of ligandable or potentially druggable proteomes, cysteine residues remain favored sites for drug-development efforts. This favoritism is driven by the cysteine's numerous functional activities[43], the availability of proven cysteine-modifying chemistries, and the established clinical efficacy of FDA-approved drugs[44–47].

Alongside this considerable progress in covalent labeling chemistries, substantial inroads have been made into improved sample preparation and data analysis workflows. Exemplifying these improvements, our recent studies have demonstrated the utility of single-pot, solid-phase enhanced sample preparation (SP3)[48,49] for achieving increased coverage using low proteome inputs[50,51]. Innovative softwares such as pLink[52,53], MSFragger[54,55] and SAGE[56] have substantially decreased data processing time. Automated processing workflows now allow for rapid preparation of samples in 96- and 384-well plate format[57–60]. substantially increased capacity to rapidly prepare large numbers of chemoproteomic samples, which is essential for screening larger compound libraries, demands equal improvements in sample acquisition speed.

Together with advances in acquisition afforded by new instrumentation[61,62], isobaric labeling is a commonly employed strategy for decreasing acquisition time. Isobaric labels, such as the commercially available isobaric tags for relative and absolute quantitation (iTRAQ)[63], tandem mass tags (TMT)[64,65], and custom reagents, such as dimethylleucine (DiLeu)[66–68] reagents, allow multiplexing of up to 21 samples at once. Most isobaric reagents feature amine-reactive groups, such as NHS-ester or triazine-ester, which incorporates the mass balancer and reporter by reacting with peptides n-termini and lysine side chains. Amine-reactive mass tags have significantly enhanced data acquisition speeds with methods such as streamlined cysteine activity-based protein profiling (SLC-ABPP)[15]. Additionally, these tags have shown widespread utility for chemoproteomic applications, including uncovering ligand-protein interactions with thermal proteome profiling (TPP)[69], screening of large compound libraries[15], discovering novel

https://doi.org/10.26434/chemrxiv-2023-0szhj **ORCID:** https://orcid.org/0000-0001-8541-1404 Content not peer-reviewed by ChemRxiv. **License:** CC BY-NC-ND 4.0

disease biomarkers[70–72], and uncovering differential protein expression in COVID-19 patients[73]. Hyperplexing with isotopically differentiated desthiobiotin reagents has achieved impressive 36-plex sample throughput[74]. These studies all rely on the same general workflow: (1) cysteine biotinylation, (2) tryptic digest, (3) enrichment and isobaric labeling, and (4) liquid chromatography-tandem mass spectrometry (LC-MS/MS) analysis. The comparatively late isobaric labeling step, which occurs after sequence specific proteolysis, is an unavoidable feature of these workflows, which introduces increased sample-sample variance and prolongs sample processing time (**Figure 1A**).

As illustrated by our own silane-based cleavable isotopically labeled proteomics (sCIP) method[75] and the recently reported azidoTMT method[76], an alternative strategy is to introduce the isobaric label earlier in sample preparation via a fully functionalized "clickable" handle that features the built-in capacity for sample enrichment. The key advance of the sCIP platform was our fully functionalized enrichment reagents that contain biotin, a chemically cleavable DADPS group, an azide for copper catalyzed azide-alkyne cycloaddition (CuAAC or "click") enrichment, and an isobaric label. Thus, sCIP allowed for incorporation of the isobaric label prior to trypsin digest, comparatively early in the sample preparation workflow. However, a limitation of the sCIP approach was its comparatively small 6-plex multiplexing. Addressing this limitation, the recently reported azidoTMT platform achieved 11-plex multiplexing with anti-TMT antibody-based peptide enrichment. Furthermore, the azidoTMT platform demonstrated improved coverage and decreased coefficient of variance when compared to prior peptide-based isobaric labeling strategy. While highly enabling, the absence of antibody based reagents for TMTPro together with reports of variable performance of the anti-TMT resin[76,77], highlight the still unmet need for robust and easily implementable enrichment-based isobaric labeling regents.

Enabled by the solid-phase compatible DADPS-Fmoc reagent that was pivotal for the synthesis of our aforementioned sCIP reagents, here we establish the sCIP-TMT platform. The

https://doi.org/10.26434/chemrxiv-2023-0szhj **ORCID:** https://orcid.org/0000-0001-8541-1404 Content not peer-reviewed by ChemRxiv. **License:** CC BY-NC-ND 4.0

sCIP-TMT platform utilizes a minimalist sCIP reagent that can be in-situ functionalized by TMT to achieve streptavidin-based cysteine chemoproteomics. In sCIP-TMT, the TMT reagents are conjugated to azide functionalized proteins via click chemistry, which allows for early sample pooling prior to proteolytic digestion (**Figure 1B**). Demonstrating the utility of sCIP-TMT, here we employed a TMT10plex™- based platform for cysteine-reactive electrophilic fragment screening, which identified >15000 cysteines on >5100 proteins across all sCIP-TMT10plex datasets. The decreased sample preparation time, compatibility with established sample preparation workflows and analysis pipelines, and anticipated compatibility with a wide range of chemical probes and scalability beyond 10-plex distinguish the sCIP-TMT platform from prior approaches.

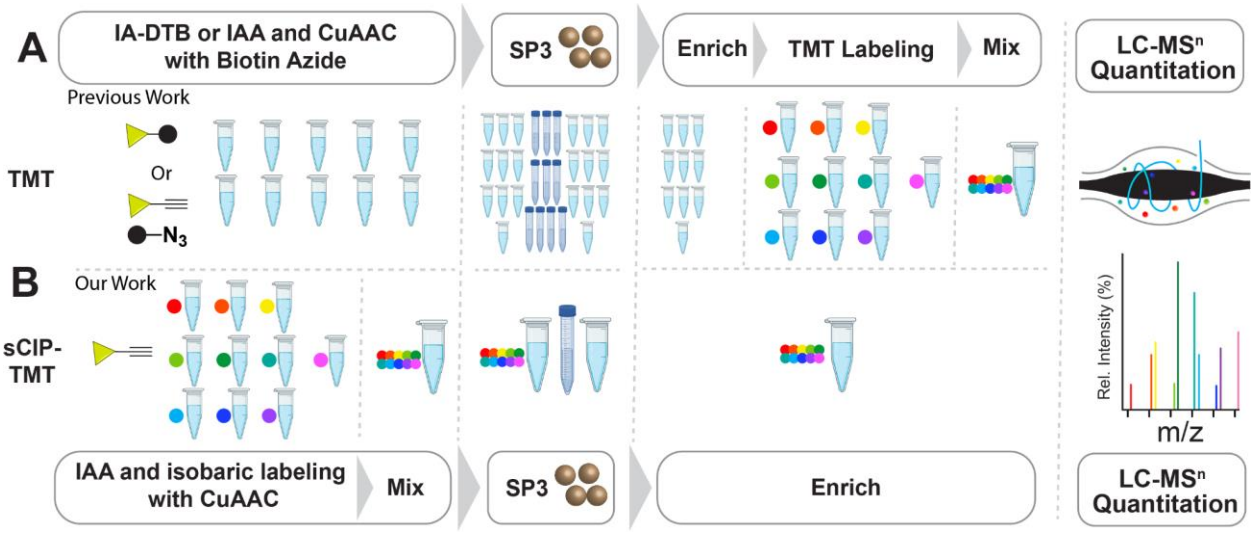

Figure 1. sCIP-TMT allows for more efficient sample preparation with less sample-to-sample variance. (A) Workflow currently used for profiling cysteines in which samples are labeled with either iodoacetamide-desthiobiotin (IA-DTB) or iodoacetamide alkyne (IAA) and conjugated to biotin azide via copper-catalyzed azide-alkyne cycloaddition (CuAAC or 'click'). After sample cleanup, using single-pot solid-phase enhanced sample-preparation (SP3), as illustrated here, or other decontamination methodologies, the samples are then subjected to sequence specific proteolytic digest, isobaric labeling, avidin enrichment sample pooling and liquid chromatography

https://doi.org/10.26434/chemrxiv-2023-0szhj **ORCID:** https://orcid.org/0000-0001-8541-1404 Content not peer-reviewed by ChemRxiv. **License:** CC BY-NC-ND 4.0

tandem mass spectrometry (LC-MS/MS) analysis. (B) Our envisioned sCIP-TMT workflow in which fully functionalized isobaric, biotin- and azide-containing reagents allow for early-stage sample pooling directly after click conjugation. Subsequently, the labeled samples can be processed and analyzed following established sample preparation workflow.

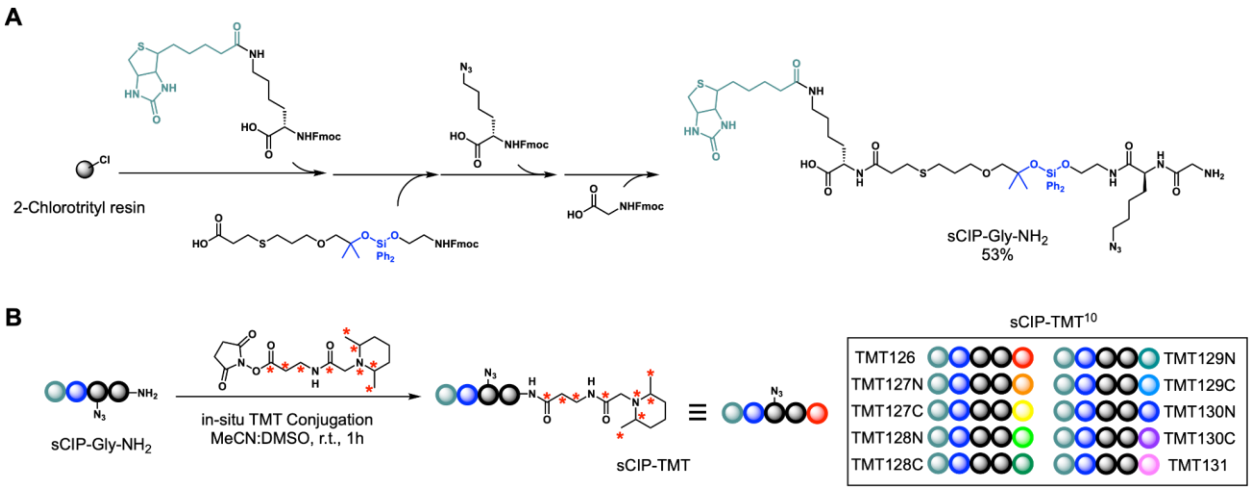

Scheme 1. (A) Solid-phase peptide synthesis enables formation of sCIP capture reagent with free n-terminus (sCIP-Gly-NH_2) in 53% yield that can be (B) used to form sCIP-TMT reagents in situ by mixing sCIP-Gly-NH_2 with TMT reagents in a 1:1 ratio at ambient temperature. This method was applied to form the sCIP-TMT conjugates with the commercially available TMT10plex™ isobaric tags.

RESULTS

Synthesis of sCIP-TMT reagents. To enable our envisioned sCIP-TMT platform, we focused first on the synthesis of a customized free-n-termini-containing sCIP reagent. Guided by the amine-based labeling strategy used to generate the Azido-TMT reagents[76], we envisioned that such a reagent could be easily subjected to late stage functionalization with commercially available activated ester reagents. Enabled by our previously described solid-phase compatible

https://doi.org/10.26434/chemrxiv-2023-0szhj **ORCID:** https://orcid.org/0000-0001-8541-1404 Content not peer-reviewed by ChemRxiv. **License:** CC BY-NC-ND 4.0

dialkoxydiphenyl silane (DADPS) building block [75], solid-phase peptide synthesis proceeded smoothly, yielding the final capture reagent (sCIP-Gly-NH_2) in 53% yield and high purity (**Scheme 1A**). Of note, glycine was included as a spacer to minimize steric hindrance and to facilitate high yield conjugation with costly isobaric reagents.

Reagent in hand, we next assessed the formation of the sCIP-isobaric conjugate by liquid chromatography-mass spectrometry (LC-MS). We selected TMT for our first-generation reagents—this isobaric reagent selection was guided by the widespread use of TMT together with reagent cost. Gratifyingly, we observed >99% conversion to the desired sCIP-TMT reagent for the reaction between TMTzero and sCIP-Gly-NH_2, with reagents mixed at 1:1 stoichiometry (**Scheme 1B** and **Figure S2**). Notably, we opted to include a short incubation with 0.5 equivalents of hydroxylamine after sCIP-TMT conjugation to quench any excess TMT reagent.

sCIP-TMTzero achieves high coverage cysteine labeling. Having demonstrated highly efficient formation of sCIP-TMTzero, we next assessed reagent performance in chemoproteomics. We selected our established cysteine profiling workflow for benchmarking[11,50,51,75,78–81]. Following the workflow shown in **Figure 1B**, cell lysates were capped with the pan-cysteine reactive iodoacetamide alkyne (**IAA**) probe followed by click conjugation to the preformed sCIP-TMTzero conjugate. After sequence specific proteolysis, enrichment, DADPS-cleavage and peptide elution (**Figure 2A**), LC-MS/MS analysis identified 3856 total proteins, 11219 total peptides and 8543 total unique cysteines (**Figure 2B**). Aggregate analysis of sCIP-TMTzero modified peptides revealed overall higher charge states when compared to unmodified peptides, likely stemming from the added mass of the modification (+633.3957 Da) and the addition of the protonatable piperidine portion of the TMT modification (**Figure S3**).

As our prior studies had revealed the formation of novel fragment ions derived from chemoproteomics modified peptides[75,78], we additionally opted to perform diagnostic ion mining analysis[82] on our sCIP-TMTzero-labeled sample. We found the TMTzero reporter (m/z 126.1277)

https://doi.org/10.26434/chemrxiv-2023-0szhj **ORCID:** https://orcid.org/0000-0001-8541-1404 Content not peer-reviewed by ChemRxiv. **License:** CC BY-NC-ND 4.0

was the dominant ion identified in nearly 100% of modified spectra, having an average intensity >80% (**Table S2**). Interestingly, this analysis also identified an additional diagnostic ion with m/z of 668.3896 that was frequently detected in modified PSMs (>97% of total PSMs), with moderate 70% mean intensity. We attributed this ion to the desulfurization of labeled cysteines (**Figure S4**), which parallels the recent report of such desulfurization for peptides labeled with electrophilic compounds[83]. Inspection of the mass spectra using FragPipe-PDV[84,85] the presence of these fragment ions with the TMT reporter being the dominant ion in nearly all spectra (**Figure 2C**).

Collision energy ramping revealed maximum relative reporter ion intensity, together with maximum peptide, cysteine, peptide, and protein coverage using higher energy c-trap dissociation (HCD) and a normalized collision energy (NCE) of 35% (**Figure 2B and 2D**). As a 36% NCE is widely reported as optimal for MS2-based TMT experiments[58,86,87], these findings support that the sCIP functionality does not substantially change the behavior of the piperidine reporter ion. Interestingly, the cysteine desulfurization ion is predominant at lower NCEs (**Figure 2E**), and the TMT reporter ion predominates above 30% NCE. The high occurrence and intensity of the TMT reporter combined with the lack of other major fragments supports the preferential release of the TMT fragment ion when compared to fragmentation at other points in the sCIP modification.

https://doi.org/10.26434/chemrxiv-2023-0szhj **ORCID:** https://orcid.org/0000-0001-8541-1404 Content not peer-reviewed by ChemRxiv. **License:** CC BY-NC-ND 4.0

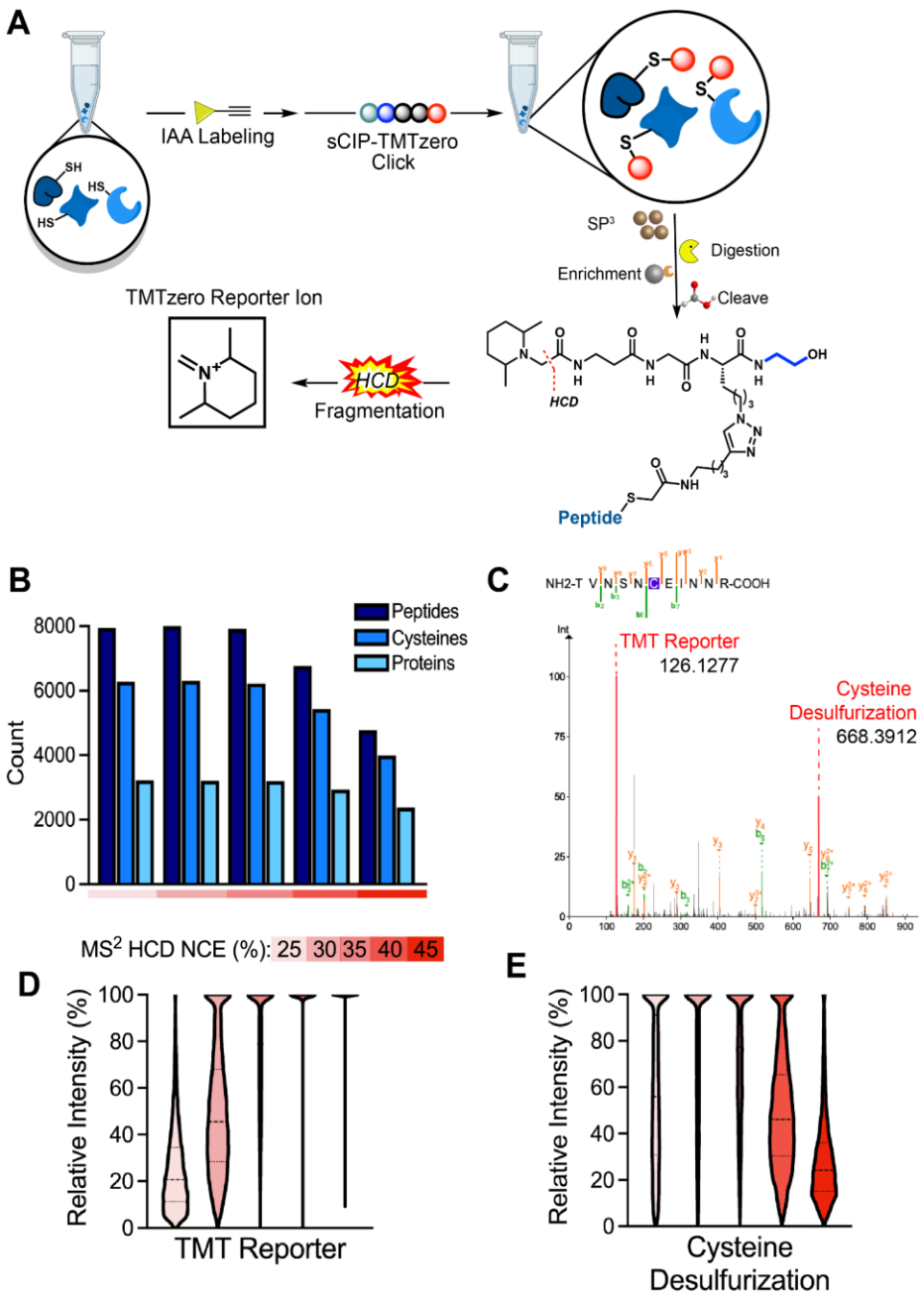

Figure 2. Defining the acquisition parameters for sCIP-TMT. (A) sCIP-TMT sample preparation workflow. Cysteines are first capped using the pan-reactive molecule iodoacetamide alkyne (IAA) and then clicked to sCIP-TMTzero (pre-formed from sCIP and TMTzero as described in **Scheme 1**). Samples are then subjected to single-pot solid-phase enhanced sample preparation (SP3), enzymatic digestion, streptavidin enrichment, and then cleaved off resin at the DADPS moiety with acid. Upon higher energy c-trap dissociation (HCD) fragmentation the TMT reporter ion can

https://doi.org/10.26434/chemrxiv-2023-0szhj **ORCID:** https://orcid.org/0000-0001-8541-1404 Content not peer-reviewed by ChemRxiv. **License:** CC BY-NC-ND 4.0

be observed in MS/MS spectra. (B) Peptide, unique cysteine, and protein coverage of sCIP-TMTzero labeled samples at varying HCD normalized collision energies (NCEs). (C) Representative spectra from sCIP-TMTzero labeled peptide visualized with FragPipe proteomics data viewer (FragPipe-PDV)[84,85] showing the TMT reporter as the dominant ion present. Relative intensity of the (D) TMT reporter ion and (E) cysteine desulfurization ion at varying HCD NCEs. For panels B-E, n=1 biological replicate per collision energy tested. All MS data can be found in **Table S2**.

sCIP-TMT10 reagents achieve high coverage and accurate quantification. Motivated by the high coverage and favorable reporter ion fragmentation observed for the sCIP-TMTzero reagent datasets, we next extended our method to TMT10Plex™. The ten sCIP-TMT conjugates were pre-formed (full reagent structures in **Figure S5**) and cysteine functionalization of cell lysates was performed using IAA and click chemistry for all ten sCIP-TMT reagents in parallel. Immediately following the click reaction, the samples were pooled and subjected to cysteine chemoproteomic sample preparation, following the workflow shown in **Figure 1B**. Consistent with our sCIP-TMTzero analysis (**Figure 2B**), high overall proteomic coverage was achieved (**Figure 3A**) for samples mixed at equimolar reagent concentrations (e.g. 1:1). This coverage, which was obtained using a 3h gradient for acquisition, is comparable to that reported for similar studies that analyzed TMT-labeling of cysteine peptides in bulk without extensive offline fractionation[15,88].

Highlighting the streamlined nature of the sCIP-TMT workflow, we anticipate a >7h reduction in sample preparation time together with decreased container usage (<86 sample containers) when compared to established 18-plex TMTpro workflows[15,19,42] (**Figure 3B and Table S4**). As TMT labeling prior to sample enrichment is a common strategy[15,19,42,89] as is the use of automated liquid handling[90], we do acknowledge that similar time savings can be achieved using these alternative and complementary strategies. Notably, our method uses comparable amounts of TMT reagent to cost-efficient TMT labeling[91].

https://doi.org/10.26434/chemrxiv-2023-0szhj **ORCID:** https://orcid.org/0000-0001-8541-1404 Content not peer-reviewed by ChemRxiv. **License:** CC BY-NC-ND 4.0

Guided by prior benchmarking of isobaric reagent performance[68,75,92], we also opted to assess the fidelity of the sCIP-TMT platform in measuring relative cysteine peptide abundance. Cysteine chemoproteomic studies are generally performed in a competitive format in which cysteine labeling sites are inferred from blockade of IAA labeling, thus we were particularly interested in vetting sCIP-TMT's capacity to quantify comparatively large fold changes. Therefore, we subjected peptides labeled with each sCIP-TMT[10] to spike-in analysis using the sample ratios indicated in **Figure 3C,D** and **Table S1**. After LC-MS/MS analysis with a high-field asymmetric waveform spectrometry (FAIMS) device[93], the sCIP-TMT spectral files were analyzed with MSFragger software using the preset TMT workflow freely available in the FragPipe GUI[54,55,94]. We observe generally high coverage of modified peptides for all labeled samples, comparable to that obtained by the established SLC-ABPP method[15]. Importantly, the measured reporter ion intensity ratios were observed to closely match the expected values. The intensity ratios centered around 1 for all 10 reporters mixed in equal ratios, and the expected ratios were additionally observed for samples mixed in 1:5:10:15 proportions.

While FAIMS acquisition has proven useful for achieving a balance between high coverage and decreased ratio compression[95,96], MS3-based analysis with synchronous precursor selection (SPS)[97,98] remains the gold-standard to isobaric analysis. Therefore, we additionally subjected our spike-in samples to SPS-MS3 analysis. Consistent with prior reports[99–101], this acquisition mode afforded a tighter ratio spread (**Figure 3D**) together with decreased cysteine peptide coverage (**Figure S7**).

https://doi.org/10.26434/chemrxiv-2023-0szhj **ORCID:** https://orcid.org/0000-0001-8541-1404 Content not peer-reviewed by ChemRxiv. **License:** CC BY-NC-ND 4.0

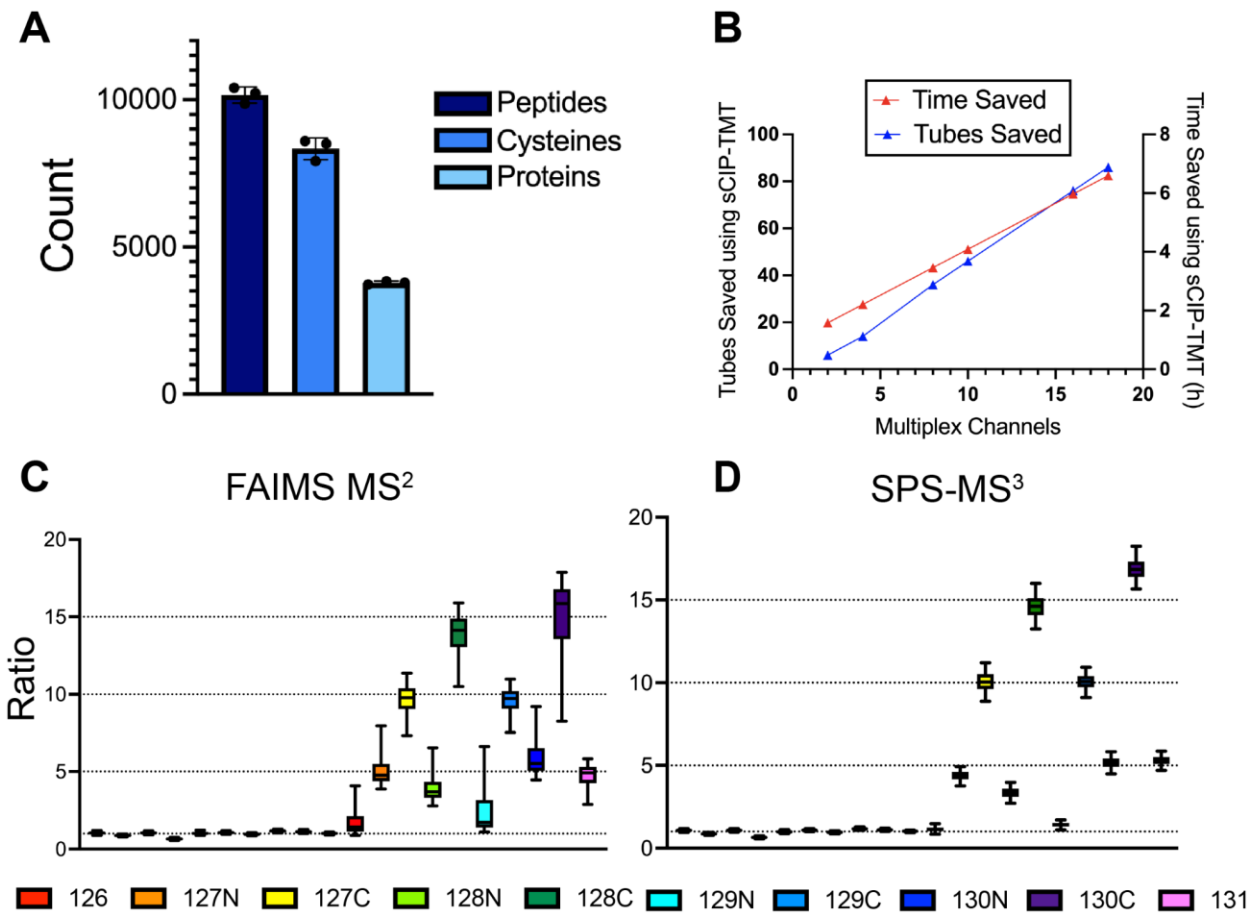

Figure 3. sCIP-TMT faithfully quantifies cysteine ratios with decreased sample preparation times. (A) Peptide, cysteine, and protein coverage of sCIP-TMT[10] labeled samples mixed 1:1 analyzed using FAIMS-MS[2]. (B) Analysis of time (hours) and tubes saved using the sCIP-TMT workflow as multiplex channels increases. (C) Comparison of ratios for samples mixed in both 1:1 and 1:5:10:15 ratios analyzed using FAIMS-MS[2]. (D) Comparison of ratios for samples mixed in both 1:1 and 1:5:10:15 ratios analyzed using SPS-MS[3]. Box plots display 5th percentile, first quartile (Q1), median, third quartile (Q3), and 95th percentile values of the sample. For panels C-E, n=3 biological replicates. All MS data can be found in **Table S3**.

sCIP-TMT identifies known and novel liganded cysteines. As cysteine chemoproteomics is widely utilized in pinpointing ligandable or potentially druggable cysteine residues, we next assess

https://doi.org/10.26434/chemrxiv-2023-0szhj **ORCID:** https://orcid.org/0000-0001-8541-1404 Content not peer-reviewed by ChemRxiv. **License:** CC BY-NC-ND 4.0

the compatibility of sCIP-TMT with screening applications. We selected four prototype electrophilic fragments (**Figure 4A**), including two chloroacetamide-containing molecules, the widely utilized **KB02**[16,42,102] and **KB10**, which we had previously found showed a substantially distinct labeling pattern and more attenuated reactivity when compared to **KB02**. We additionally selected methylphenyl propiolate (**MPP**) and methyl cinnamate (**MC**), as our recent study had revealed distinct proteomic reactivity for each molecule, with MPP functioning as a potent cysteine protease inhibitor whereas MPA showed negligible protease inhibitory activity[81].

HEK293T cell lysates were subjected to either vehicle (DMSO) or each compound (500 µM) in duplicate. Compound treatments were performed in cell lysates to avoid the recently reported pervasive protein aggregation observed in cell-based analysis using comparatively high doses of electrophilic compounds[80]. After treatment the lysates were subjected to our sCIP-TMT workflow (**Figure 1B and Figure S8**). In total, 10733 cysteine peptides corresponding to 8515 unique cysteines, and 3787 proteins were identified (**Figure S9**). The vast majority (>96%) of enriched peptides harbored the sCIP modification, consistent with efficient capture of labeled peptides. 789 high confidence cysteines were detected with $\log_2$ ratios >1 for at least one compound, consistent with covalent modification at these sites.

We next asked whether specific targets and SAR reported by our sCIP-TMT dataset could add to the burgeoning set of available cysteine chemoproteomic datasets. We were particularly interested in three aspects of our dataset: (1) Corroborating prior reports of cysteine ligandability; (2) de novo identification of ligandable cysteines; and (3) assessing the proteome-wide reactivity of different cysteine-reactive electrophiles.

Comparison to our previous dataset generated using **KB02** and MS1-based quantification revealed substantial overlap between the cysteines identified by both approaches (**Figure S10**) together with high concordance (r^2 = 0.63) in the measured ratios, with some unavoidable ratio compression observed for the sCIP-TMT dataset (**Figure 4B**), which was acquired using FAIMS-MS2. Further supporting the fidelity of the sCIP-TMT platform, we observe a similarly high

https://doi.org/10.26434/chemrxiv-2023-0szhj **ORCID:** https://orcid.org/0000-0001-8541-1404 Content not peer-reviewed by ChemRxiv. **License:** CC BY-NC-ND 4.0

concordance between our sCIP-TMT **KB02** ligandability ratios and those reported by prior studies[15,16,19,103], as aggregated in the human cysteine database (CysDB)[102] similarly revealed consistent ratios (**Figure S11**). Exemplifying established labeling sites, we observe that GSTO1 Cys32 was labeled to near completion by both **KB02** and **KB10**, consistent with the high ligandability of this cysteine, as reported by a number of previous studies[15,16,19,104](**Figure 4C**). Additional targets that proved highly consistent with prior reports include Creatine Kinase Cys283[105], which is an established target of **KB02** and related analogues, and PIN1 Cys113, for which several highly potent inhibitors have been reported[106,107]. Taken together these findings provide compelling evidence that sCIP-TMT faithfully captures cysteine ligandability sites.

Looking beyond established covalent modification sites, we next asked whether our platform could capture novel ligandable cysteines. Strikingly, nearly all the liganded cysteines (760/789) had been previously identified by CysDB (**Figure S12**). Despite this high degree of dataset overlap, 29 cysteines were uniquely identified as liganded with sCIP-TMT. Exemplary novel liganded sites include BMP-binding endothelial regulator protein (BMPER) Cys189 and Akirin-2 Cys3, with the latter located proximal to the 20S proteasome binding motif[108]. These findings illustrate the continued opportunities for expanding coverage of the cysteinome, although comparatively modest gains are expected from continued re-sampling of similar cell line models.

The modest four-member compound library assayed here was selected to include a diverse set of electrophiles, which we expected to show distinct proteome-wide reactivity and target engagement profiles. To test this hypothesis, we next compared both the relative proteome-reactivity of each compound member (assessed based on the fraction of total cysteines with log2 ratios >1) and the SAR of our library members across the proteome. Quantification of the percent of total cysteines with log2 ratios >1 for each compound, which is an established proxy for overall compound reactivity, revealed the generally high reactivity of the chloroacetamide-containing compound **KB02,** which liganded 11.4% of total cysteines. Consistent with our prior findings[16] that the chloroacetamide-containing compound **KB10** exhibits more tempered cysteine reactivity,

https://doi.org/10.26434/chemrxiv-2023-0szhj **ORCID:** https://orcid.org/0000-0001-8541-1404 Content not peer-reviewed by ChemRxiv. **License:** CC BY-NC-ND 4.0

3.6% of cysteines liganded by this compound in our sCIP-TMT dataset (**Figure 4C**). Unlike the **MC** molecule, which showed very attenuated proteome-wide reactivity (liganding 0.2% of all detected cysteines), MPP shows comparable cysteine reactivity to KB10, engaging 3.8% of all cysteines (**Figure 4C**). Consistent with our prior observation that MPP engages cysteines typically labeled by chloroacetamides[81], we observe >85% of cysteines engaged by MPP are also engaged by KB02 or KB10 (**Figure S13**). The capacity of MPP to engage cysteines labeled by chloroacetamides is further exemplified glutathione S-transferase omega 1 (GSTO1) Cys32; notably our previous work had revealed a strong bias for Cys32 reacting with chloroacetamide compared with acrylamide electrophiles[102] . Despite the high overlap between liganded targets (**Figure S13**), we do observe 493 total cysteines that are uniquely modified by only a single compound. Exemplary cysteines that show strong scaffold-dependent SAR include Phosphoribosylformylglycinamidine synthase (PFAS) Cys270 and DNA ligase 3 (LIG3) Cys929 uniquely labeled by **KB10** and Calpain-2 catalytic subunit (CAPN2) Cys301 and Transducin-like enhancer protein 1 (TLE1) Cys526 uniquely labeled by MPP (**Figure 4D**).

https://doi.org/10.26434/chemrxiv-2023-0szhj **ORCID:** https://orcid.org/0000-0001-8541-1404 Content not peer-reviewed by ChemRxiv. **License:** CC BY-NC-ND 4.0

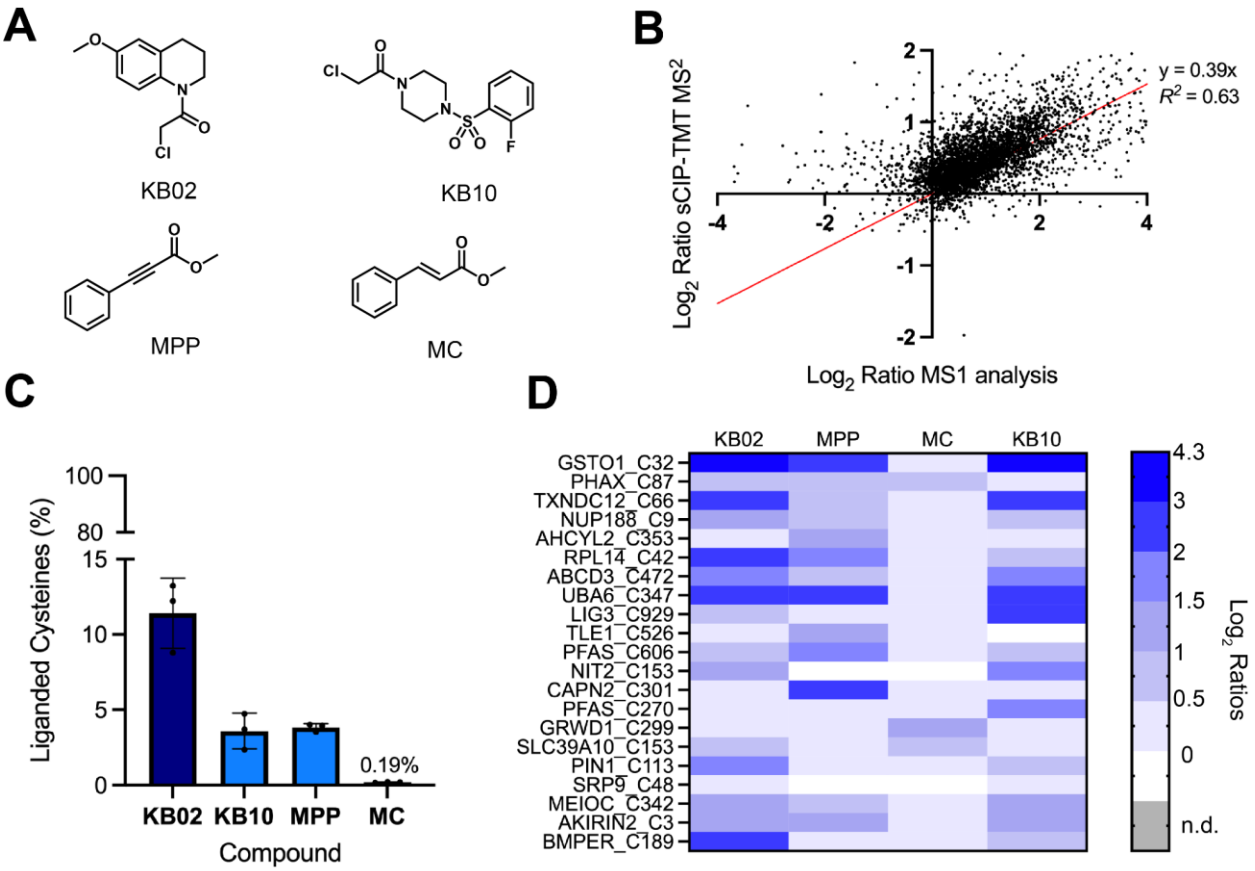

Figure 4. sCIP-TMT is compatible with small-molecule electrophile screening. (A) Structures of electrophilic fragments analyzed by sCIP-TMT10. (B) Comparison of the Log2 ratios for cysteines identified using MS1 analysis as previously reported[75] (x-axis) versus sCIP-TMT (y-axis) with scout fragment **KB02**. (C) Reactivity ratio for each compound calculated as the number of liganded cysteines for each compound out of the total number of cysteines. (D) Heat map showing structure activity relationship of the four compounds across a panel of cysteines. Gray boxes indicate no ratio due to no channel intensities. For panels B-D, n=3 biological replicates. All MS data can be found in **Table S4**.

https://doi.org/10.26434/chemrxiv-2023-0szhj **ORCID:** https://orcid.org/0000-0001-8541-1404 Content not peer-reviewed by ChemRxiv. **License:** CC BY-NC-ND 4.0

DISCUSSION

Here we report the sCIP-TMT platform, which enables high throughput and high coverage cysteine chemoproteomics. To build sCIP-TMT, we first synthesized a customized sCIP-Gly-NH_2 reagent via solid-phase peptide synthesis (SPPS) that contains a biotin, a chemically cleavable DADPS linkage, azide group and, most importantly, a free amine at the n-terminus of the reagent. The presence of this latter moiety allows for straightforward conjugation with commercially available isobaric labeling reagents. Enabled by sCIP-Gly-NH_2, we obtained and deployed a 10plex set of sCIP-TMT[10] reagents for cysteine chemoproteomics, identifying >15000 total cysteine residues. We find that the sCIP-TMT[10] platform is compatible with fragment electrophile screening, as demonstrated by our rich datasets of cysteines liganded by the widely utilized scout fragment **KB02**[15,16,19,104] and electrophilic fragments with more tempered proteome-wide reactivities. Notably, our cysteine chemoproteomic studies reveal that the cysteines labeled by the thio-Michael acceptor **MPP** fragment shows substantial overlap with those labeled by chloroacetamide fragments **KB02** and **KB10** (**Figure S13**), which provides evidence in support of this chemotype as uniquely suited to bridging the chloroacetamide-acrylamide divide. The high accuracy of sCIP-TMT is illustrated by the robust identification of established ligandable cysteine residues, as illustrated by high concordance with our prior studies and those reported in CysDB[16,75,102] (**Figures 4B** and **S11**).

sCIP-TMT offers several important advantages when compared to prior chemoproteomic platforms. The sCIP-TMT workflow's key feature is the early sample pooling, which occurs immediately after click conjugation. While such protein-level sample pooling is common in chemoproteomic platforms that rely on MS1-based quantification[7,13,41,109], nearly all isobaric-reagent based platforms[15,19,42], with the exception of the aforementioned azidoTMT and anti-TMT approaches, samples are combined after sequence specific proteolysis. Thus sCIP-TMT substantially streamlines sample preparation compared to these prior methods, as demonstrated by both reduced number of containers and reduced hours of active sample preparation time

https://doi.org/10.26434/chemrxiv-2023-0szhj **ORCID:** https://orcid.org/0000-0001-8541-1404 Content not peer-reviewed by ChemRxiv. **License:** CC BY-NC-ND 4.0

(**Figures 1 and 3B**). We expect that sCIP-TMT should also reduce sample-to-sample variance, as was recently demonstrated for the azido-TMT platform[76]. Distinct from the azido-TMT and related iodo-TMT[110,111] workflows that require anti-TMT antibody for enrichment, sCIP-TMT is compatible with established avidin-based enrichment platforms. As demonstrated by the recent comparison of chemically cleavable linkers[112], the DADPS moiety used in the sCIP-TMT reagents stands out for its high proteome coverage and compatibility with mild acid elution. The off-the-shelf compatibility of the sCIP-TMT approach with established data acquisition and analysis pipelines used for TMT and related isobaric labeling strategies obviates requirements for customized software, such as those required for our prior generation of sCIP reagents[75]. Enabled by these many useful features, we expect widespread utility for sCIP-TMT.

Looking beyond our current study, we envision several immediate use cases for sCIP-TMT. First, while our study used TMT10, expanding to 18plex multiplexing, by conjugating our sCIP-Gly-NH_2 reagent with TMTpro, should easily enhance the multiplexing capabilities of the sCIP platform. As illustrated by the recently reported chemoproteomic hyperplexing platform[74], we also expect that incorporation of stable isotopes into our sCIP-Gly-NH_2 reagent through SPPS would allow for preparation of multiple isobaric sets and similarly efficient hyperplexing. Such hyperplexing strategies will undoubtedly benefit from off-line fractionation to achieve ultra-deep coverage of the proteome, as has been reported for the SLC-ABPP and TMTpro-based platforms[15]. Beyond cysteine chemoproteomics we also foresee compatibility with other nucleophilic and electrophilic residues for which alkyne-containing probes are available, including lysine[17,30–32], Tyrosine[31,33,34], methionine[35,36], histidine[113,114], tryptophan[115], aspartate and glutamate[37,116], phosphoaspartate[117,118] together with promiscuously-reactive probes[26,119].

https://doi.org/10.26434/chemrxiv-2023-0szhj **ORCID:** https://orcid.org/0000-0001-8541-1404 Content not peer-reviewed by ChemRxiv. **License:** CC BY-NC-ND 4.0

ACKNOWLEDGMENT

This study was supported by a 2021 Nobel Family Innovation Fund Seed Project Award (K.M.B), DOD-Advanced Research Projects Agency (DARPA) D19AP00041 (K.M.B.), National Institutes of Health DP2 OD030950-01 (K.M.B.), National Institute of General Medical Sciences T32 GM067555-11 (N.R.B). We thank all members of the Backus lab for helpful suggestions as well as the UCLA Proteome Research Center for assistance with mass spectrometry-based proteomic data collection.

Author Contributions

N.R.B. and K.M.B. conceived of the project. N.R.B. performed all experiments and collected and processed all the data. N.R.B. and K.M.B wrote the manuscript.

Conflicts of Interest

The authors declare no financial or commercial conflict of interest.

ASSOCIATED CONTENT

Detailed methods of chemical synthesis and chemoproteomic sample preparation; Supplementary figures and tables (PDF)

Aggregated datasets for each result section (xlsx)

Mass spectrometry data files are available in the PRIDE repository: PXD044050

https://doi.org/10.26434/chemrxiv-2023-0szhj **ORCID:** https://orcid.org/0000-0001-8541-1404 Content not peer-reviewed by ChemRxiv. **License:** CC BY-NC-ND 4.0

REFERENCES

1. Toriki, E. S. *et al.* Rational Chemical Design of Molecular Glue Degraders. *ACS Cent. Sci.* **9**, 915–926 (2023).
2. Guo, W. H. *et al.* Enhancing intracellular accumulation and target engagement of PROTACs with reversible covalent chemistry. *Nat. Commun.* **11**, 1–16 (2020).
3. Zhang, X., Crowley, V. M., Wucherpfennig, T. G., Dix, M. M. & Cravatt, B. F. Electrophilic PROTACs that degrade nuclear proteins by engaging DCAF16. *Nat. Chem. Biol.* **15**, 737–746 (2019).
4. Tao, Y. *et al.* Targeted Protein Degradation by Electrophilic PROTACs that Stereoselectively and Site-Specifically Engage DCAF1. *J. Am. Chem. Soc.* **144**, 18688–18699 (2022).
5. Luo, M. *et al.* Chemoproteomics-enabled discovery of covalent RNF114-based degraders that mimic natural product function. *Cell Chem. Biol.* **28**, 559-566.e15 (2021).
6. Słabicki, M. *et al.* Small-molecule-induced polymerization triggers degradation of BCL6. *Nature* **588**, 164–168 (2020).
7. Zanon, P. R. A., Lewald, L. & Hacker, S. M. Isotopically Labeled Desthiobiotin Azide (isoDTB) Tags Enable Global Profiling of the Bacterial Cysteinome. *Angew. Chemie - Int. Ed.* **59**, 2829–2836 (2020).
8. Shi, Y. *et al.* Thiol-based chemical probes exhibit antiviral activity against SARS-CoV-2 via allosteric disulfide disruption in the spike glycoprotein. *Proc. Natl. Acad. Sci. U. S. A.* **119**, e2120419119 (2022).
9. Liu, Y. *et al.* Autoregulatory control of mitochondrial glutathione homeostasis. *Science (80-.).* (2023) doi:10.1126/science.adf4154.
10. Xiao, H. *et al.* A Quantitative Tissue-Specific Landscape of Protein Redox Regulation

https://doi.org/10.26434/chemrxiv-2023-0szhj **ORCID:** https://orcid.org/0000-0001-8541-1404 Content not peer-reviewed by ChemRxiv. **License:** CC BY-NC-ND 4.0

during Aging. *Cell* **180**, 968-983.e24 (2020).

11. Yan, T. *et al.* Proximity-labeling chemoproteomics defines the subcellular cysteinome and inflammation-responsive mitochondrial redoxome. *Cell Chem. Biol.* **30**, 811-827.e7 (2023).
12. Meng, J. *et al.* Global profiling of distinct cysteine redox forms reveals wide-ranging redox regulation in C. elegans. *Nat. Commun.* **12**, 1–13 (2021).
13. Desai, H. S. *et al.* SP3-Enabled Rapid and High Coverage Chemoproteomic Identification of Cell-State–Dependent Redox-Sensitive Cysteines. *Mol. Cell. Proteomics* **21**, 100218 (2022).
14. Yan, T., Boatner, L. M., Cui, L., Tontonoz, P. & Backus, K. M. Defining the Cell Surface Cysteinome using Two-step Enrichment Proteomics. *bioRxiv* (2023) doi:https://doi.org/10.1101/2023.10.17.562832.
15. Kuljanin, M. *et al.* Reimagining high-throughput profiling of reactive cysteines for cell-based screening of large electrophile libraries. *Nat. Biotechnol.* **39**, 630–641 (2021).
16. Backus, K. M. *et al.* Proteome-wide covalent ligand discovery in native biological systems. *Nature* **534**, 570–574 (2016).
17. Hacker, S. M. *et al.* Global profiling of lysine reactivity and ligandability in the human proteome. *Nat. Chem.* **9**, 1181–1190 (2017).
18. Resnick, E. *et al.* Rapid Covalent-Probe Discovery by Electrophile-Fragment Screening. *J. Am. Chem. Soc.* **141**, 8951–8968 (2019).
19. Vinogradova, E. V. *et al.* An Activity-Guided Map of Electrophile-Cysteine Interactions in Primary Human T Cells. *Cell* **182**, 1009-1026.e29 (2020).
20. Gao, J., Mfuh, A., Amako, Y. & Woo, C. M. Small Molecule Interactome Mapping by Photoaffinity Labeling Reveals Binding Site Hotspots for the NSAIDs. *J. Am. Chem. Soc.* **140**, 4259–4268 (2018).
21. Miyamoto, D. K., Flaxman, H. A., Wu, H. Y., Gao, J. & Woo, C. M. Discovery of a

https://doi.org/10.26434/chemrxiv-2023-0szhj **ORCID:** https://orcid.org/0000-0001-8541-1404 Content not peer-reviewed by ChemRxiv. **License:** CC BY-NC-ND 4.0

Celecoxib Binding Site on Prostaglandin e Synthase (PTGES) with a Cleavable Chelation-Assisted Biotin Probe. *ACS Chem. Biol.* **14**, 2527–2532 (2019).

22. Tang, J. *et al.* Synthesis of portimines reveals the basis of their anti-cancer activity. *Nature* **622**, 507–513 (2023).
23. Mons, E. *et al.* The Alkyne Moiety as a Latent Electrophile in Irreversible Covalent Small Molecule Inhibitors of Cathepsin K. *J. Am. Chem. Soc.* **141**, 3507–3514 (2019).
24. Byun, D. P. *et al.* Covalent Inhibition by a Natural Product-Inspired Latent Electrophile. *J. Am. Chem. Soc.* **145**, 11097–11109 (2023).
25. Wang, Y. *et al.* Expedited mapping of the ligandable proteome using fully functionalized enantiomeric probe pairs. *Nat. Chem.* **11**, 1113–1123 (2019).
26. Zanon, P. R. A. *et al.* Profiling the Proteome-Wide Selectivity of Diverse Electrophiles. *chemRxiv* (2021) doi:10.26434/CHEMRXIV.14186561.V1.
27. Simon, G. M. & Cravatt, B. F. Activity-based proteomics of enzyme superfamilies: Serine hydrolases as a case study. *J. Biol. Chem.* **285**, 11051–11055 (2010).
28. Shenoy, V. M. *et al.* Chemoproteomic Identification of Serine Hydrolase RBBP9 as a Valacyclovir-Activating Enzyme. *Mol. Pharm.* **17**, 1706–1714 (2020).
29. Li, W., Blankman, J. L. & Cravatt, B. F. A functional proteomic strategy to discover inhibitors for uncharacterized hydrolases. *J. Am. Chem. Soc.* **129**, 9594–9595 (2007).
30. Bracken, A. K. *et al.* Biomimetic Synthesis and Chemical Proteomics Reveal the Mechanism of Action and Functional Targets of Phloroglucinol Meroterpenoids. *bioRxiv* (2023) doi:https://doi.org/10.26434/chemrxiv-2023-snx9h.
31. Chen, Y. *et al.* Direct mapping of ligandable tyrosines and lysines in cells with chiral sulfonyl fluoride probes. *Nat. Chem.* (2023) doi:10.1038/s41557-023-01281-3.
32. Abbasov, M. E. *et al.* A proteome-wide atlas of lysine-reactive chemistry. *Nat. Chem.* **13**, 1081–1092 (2021).
33. Hahm, H. S. *et al.* Global targeting of functional tyrosines using sulfur-triazole exchange

https://doi.org/10.26434/chemrxiv-2023-0szhj **ORCID:** https://orcid.org/0000-0001-8541-1404 Content not peer-reviewed by ChemRxiv. **License:** CC BY-NC-ND 4.0

chemistry. *Nat. Chem. Biol.* **16**, 150–159 (2020).

34. Mortenson, D. E. *et al.* 'inverse Drug Discovery' Strategy to Identify Proteins That Are Targeted by Latent Electrophiles As Exemplified by Aryl Fluorosulfates. *J. Am. Chem. Soc.* **140**, 200–210 (2018).

35. Lin, S. *et al.* Redox-based reagents for chemoselective methionine bioconjugation. *Science (80-.).* **355**, 597–602 (2017).

36. Gonzalez-Valero, A. *et al.* An Activity-Based Oxaziridine Platform for Identifying and Developing Covalent Ligands for Functional Allosteric Methionine Sites: Redox-Dependent Inhibition of Cyclin-Dependent Kinase 4. *J. Am. Chem. Soc.* **144**, 22890–22901 (2022).

37. Bach, K., Beerkens, B. L. H., Zanon, P. R. A. & Hacker, S. M. Light-Activatable, 2,5-Disubstituted Tetrazoles for the Proteome-wide Profiling of Aspartates and Glutamates in Living Bacteria. *ACS Cent. Sci.* (2020) doi:10.1021/acscentsci.9b01268.

38. Ma, N. *et al.* 2 H-Azirine-Based Reagents for Chemoselective Bioconjugation at Carboxyl Residues Inside Live Cells. *J. Am. Chem. Soc.* **142**, 6051–6059 (2020).

39. Cheng, K. *et al.* Tetrazole-Based Probes for Integrated Phenotypic Screening, Affinity-Based Proteome Profiling, and Sensitive Detection of a Cancer Biomarker. *Angew. Chemie - Int. Ed.* **56**, 15044–15048 (2017).

40. Thompson, D. A., Ng, R. & Dawson, P. E. Arginine selective reagents for ligation to peptides and proteins. *J. Pept. Sci.* **22**, 311–319 (2016).

41. Weerapana, E. *et al.* Quantitative reactivity profiling predicts functional cysteines in proteomes. *Nature* **468**, 790–797 (2010).

42. Takahashi, M. *et al.* DrugMap: A quantitative pan-cancer analysis of cysteine ligandability. *bioRxiv* (2023) doi:https://doi.org/10.1101/2023.10.20.563287.

43. Bak, D. W., Bechtel, T. J., Falco, J. A. & Weerapana, E. Cysteine reactivity across the subcellular universe. *Curr. Opin. Chem. Biol.* **48**, 96–105 (2019).

https://doi.org/10.26434/chemrxiv-2023-0szhj **ORCID:** https://orcid.org/0000-0001-8541-1404 Content not peer-reviewed by ChemRxiv. **License:** CC BY-NC-ND 4.0

44. Canon, J. *et al.* The clinical KRAS(G12C) inhibitor AMG 510 drives anti-tumour immunity. *Nature* **575**, 217–223 (2019).

45. Lanman, B. A. *et al.* Discovery of a Covalent Inhibitor of KRAS G12C (AMG 510) for the Treatment of Solid Tumors. *J. Med. Chem.* **63**, 52–65 (2020).

46. Sequist, L. V. *et al.* Phase III Study of Afatinib or Cisplatin Plus Pemetrexed in Patients With Metastatic Lung Adenocarcinoma With EGFR Mutations. *J. Clin. Oncol.* **31**, 3327–3334 (2013).

47. Herman, S. E. M. *et al.* Bruton tyrosine kinase represents a promising therapeutic target for treatment of chronic lymphocytic leukemia and is effectively targeted by PCI-32765. *Blood* **117**, 6287–6296 (2011).

48. Hughes, C. S. *et al.* Single-pot, solid-phase-enhanced sample preparation for proteomics experiments. *Nat. Protoc.* **14**, 68–85 (2019).

49. Hughes, C. S. *et al.* Ultrasensitive proteome analysis using paramagnetic bead technology. *Mol. Syst. Biol.* **10**, (2014).

50. Desai, H. S., Yan, T. & Backus, K. M. SP3-FAIMS-Enabled High-Throughput Quantitative Profiling of the Cysteinome. *Curr. Protoc.* **2**, 1–31 (2022).

51. Yan, T. *et al.* SP3-FAIMS Chemoproteomics for High-Coverage Profiling of the Human Cysteinome**. *ChemBioChem* **22**, 1841–1851 (2021).

52. Yang, B. *et al.* Identification of cross-linked peptides from complex samples. *Nat. Methods* **9**, 904–906 (2012).

53. Chen, Z.-L. *et al.* A high-speed search engine pLink 2 with systematic evaluation for proteome-scale identification of cross-linked peptides. *Nat. Commun.* **10**, 3404 (2019).

54. Kong, A. T., Leprevost, F. V., Avtonomov, D. M., Mellacheruvu, D. & Nesvizhskii, A. I. MSFragger: Ultrafast and comprehensive peptide identification in mass spectrometry-based proteomics. *Nat. Methods* **14**, 513–520 (2017).

55. Teo, G. C., Polasky, D. A., Yu, F. & Nesvizhskii, A. I. Fast Deisotoping Algorithm and Its

https://doi.org/10.26434/chemrxiv-2023-0szhj **ORCID:** https://orcid.org/0000-0001-8541-1404 Content not peer-reviewed by ChemRxiv. **License:** CC BY-NC-ND 4.0

Implementation in the MSFragger Search Engine. *J. Proteome Res.* **20**, 498–505 (2021).

56. Lazear, M. R. Sage: An Open-Source Tool for Fast Proteomics Searching and Quantification at Scale. *J. Proteome Res.* (2023) doi:10.1021/acs.jproteome.3c00486.

57. Becker, T. *et al.* Transforming Chemical Proteomics Enrichment into a High-Throughput Method Using an SP2E Workflow. *JACS Au* **2**, 1712–1723 (2022).

58. Eberl, H. C. *et al.* Chemical proteomics reveals target selectivity of clinical Jak inhibitors in human primary cells. *Sci. Rep.* **9**, 14159 (2019).

59. Savitski, M. M. *et al.* Multiplexed Proteome Dynamics Profiling Reveals Mechanisms Controlling Protein Homeostasis. *Cell* **173**, 260-274.e25 (2018).

60. Matzinger, M., Müller, E., Dürnberger, G., Pichler, P. & Mechtler, K. Robust and Easy-to-Use One-Pot Workflow for Label-Free Single-Cell Proteomics. *Anal. Chem.* **95**, 4435–4445 (2023).

61. Heil, L. R. *et al.* Evaluating the Performance of the Astral Mass Analyzer for Quantitative Proteomics Using Data-Independent Acquisition. *J. Proteome Res.* **22**, 3290–3300 (2023).

62. Shuken, S. R. *et al.* Deep Proteomic Compound Profiling with the Orbitrap Ascend Tribrid Mass Spectrometer Using Tandem Mass Tags and Real-Time Search. *Anal. Chem.* **95**, 15180–15188 (2023).

63. Ross, P. L. *et al.* Multiplexed protein quantitation in Saccharomyces cerevisiae using amine-reactive isobaric tagging reagents. *Mol. Cell. Proteomics* **3**, 1154–1169 (2004).

64. Thompson, A. *et al.* Tandem mass tags: A novel quantification strategy for comparative analysis of complex protein mixtures by MS/MS. *Anal. Chem.* **75**, 1895–1904 (2003).

65. Li, J. *et al.* TMTpro reagents: a set of isobaric labeling mass tags enables simultaneous proteome-wide measurements across 16 samples. *Nat. Methods* **17**, 399–404 (2020).

66. Xiang, F., Ye, H., Chen, R., Fu, Q. & Li, L. N , N -Dimethyl Leucines as Novel Isobaric Tandem Mass Tags for Quantitative Proteomics and Peptidomics. *Anal. Chem.* **82**, 2817–

https://doi.org/10.26434/chemrxiv-2023-0szhj **ORCID:** https://orcid.org/0000-0001-8541-1404 Content not peer-reviewed by ChemRxiv. **License:** CC BY-NC-ND 4.0

2825 (2010).

67. Zhang, J., Wang, Y. & Li, S. Deuterium Isobaric Amine-Reactive Tags for Quantitative Proteomics. *Anal. Chem.* **82**, 7588–7595 (2010).

68. Frost, D. C., Feng, Y. & Li, L. 21-plex DiLeu Isobaric Tags for High-Throughput Quantitative Proteomics. *Anal. Chem.* **92**, 8228–8234 (2020).

69. Savitski, M. M. *et al.* Tracking cancer drugs in living cells by thermal profiling of the proteome. *Science (80-.).* **346**, (2014).

70. Cunningham, R., Ma, D. & Li, L. Mass spectrometry-based proteomics and peptidomics for systems biology and biomarker discovery. *Front. Biol. (Beijing).* **7**, 313–335 (2012).

71. Westbrook, J. A., Noirel, J., Brown, J. E., Wright, P. C. & Evans, C. A. Quantitation with chemical tagging reagents in biomarker studies. *PROTEOMICS – Clin. Appl.* **9**, 295–300 (2015).

72. Yang, X.-L. *et al.* Quantitative proteomics characterization of cancer biomarkers and treatment. *Mol. Ther. - Oncolytics* **21**, 255–263 (2021).

73. Shen, B. *et al.* Proteomic and Metabolomic Characterization of COVID-19 Patient Sera. *Cell* **182**, 59-72.e15 (2020).

74. Budayeva, H. G., Ma, T. P., Wang, S., Choi, M. & Rose, C. M. Increasing the Throughput and Reproducibility of Activity-Based Proteome Profiling Studies with Hyperplexing and Intelligent Data Acquisition. *bioRxiv* 2023.09.13.557589 (2023).

75. Burton, N. R. *et al.* Solid-Phase Compatible Silane-Based Cleavable Linker Enables Custom Isobaric Quantitative Chemoproteomics. *J. Am. Chem. Soc.* **145**, 21303–21318 (2023).

76. Ma, T. P. *et al.* AzidoTMT Enables Direct Enrichment and Highly Multiplexed Quantitation of Proteome-Wide Functional Residues. *J. Proteome Res.* (2023) doi:10.1021/acs.jproteome.2c00703.

77. Qu, Z. *et al.* Proteomic Quantification and Site-Mapping of S -Nitrosylated Proteins Using

https://doi.org/10.26434/chemrxiv-2023-0szhj **ORCID:** https://orcid.org/0000-0001-8541-1404 Content not peer-reviewed by ChemRxiv. **License:** CC BY-NC-ND 4.0

Isobaric iodoTMT Reagents. *J. Proteome Res.* **13**, 3200–3211 (2014).

78. Yan, T. *et al.* Enhancing Cysteine Chemoproteomic Coverage through Systematic Assessment of Click Chemistry Product Fragmentation. *Anal. Chem.* **94**, 3800–3810 (2022).

79. Cao, J. *et al.* Multiplexed CuAAC Suzuki–Miyaura Labeling for Tandem Activity-Based Chemoproteomic Profiling. *Anal. Chem.* **93**, 2610–2618 (2021).

80. Julio, A. R., Shikwana, F., Truong, C. & Burton, N. R. Pervasive aggregation and depletion of host and viral proteins in response to cysteine-reactive electrophilic compounds. *bioRxiv* (2023) doi:https://doi.org/10.1101/2023.10.30.564067.

81. Castellón, J. O. *et al.* Chemoproteomics identifies proteoform-selective caspase-2 inhibitors. *bioRxiv* **90095**, 1–30 (2023).

82. Geiszler, D. J., Polasky, D. A., Yu, F. & Nesvizhskii, A. I. Mining for ions: diagnostic feature detection in MS/MS spectra of post-translationally modified peptides. *bioRxiv* (2022).

83. Ficarro, S. B. *et al.* Leveraging Gas-Phase Fragmentation Pathways for Improved Identification and Selective Detection of Targets Modified by Covalent Probes. *Anal. Chem.* **88**, 12248–12254 (2016).

84. Li, K., Vaudel, M., Zhang, B., Ren, Y. & Wen, B. PDV: An integrative proteomics data viewer. *Bioinformatics* **35**, 1249–1251 (2019).

85. Yu, F. *et al.* Analysis of DIA proteomics data using MSFragger-DIA and FragPipe computational platform. *Nat. Commun.* **14**, 4154 (2023).

86. Sun, H. *et al.* Evaluation of a Pooling Chemoproteomics Strategy with an FDA-Approved Drug Library. *Biochemistry* **62**, 624–632 (2023).

87. Sun, H. *et al.* 29-Plex tandem mass tag mass spectrometry enabling accurate quantification by interference correction. *Proteomics* **22**, (2022).

88. Liu, W. *et al.* Lactate regulates cell cycle by remodelling the anaphase promoting

https://doi.org/10.26434/chemrxiv-2023-0szhj **ORCID:** https://orcid.org/0000-0001-8541-1404 Content not peer-reviewed by ChemRxiv. **License:** CC BY-NC-ND 4.0

complex. *Nature* **616**, 790–797 (2023).

89. Zhang, J. *et al.* Systematic identification of anticancer drug targets reveals a nucleus-to-mitochondria ROS-sensing pathway. *Cell* **186**, 2361-2379.e25 (2023).

90. Mun, D.-G. *et al.* Automated Sample Preparation Workflow for Tandem Mass Tag-Based Proteomics. *J. Am. Soc. Mass Spectrom.* **34**, 2087–2092 (2023).

91. Zecha, J. *et al.* TMT Labeling for the Masses: A Robust and Cost-efficient, In-solution Labeling Approach. *Mol. Cell. Proteomics* **18**, 1468–1478 (2019).

92. Frost, D. C., Greer, T. & Li, L. High-Resolution Enabled 12-Plex DiLeu Isobaric Tags for Quantitative Proteomics. *Anal. Chem.* **87**, 1646–1654 (2015).

93. Guevremont, R. High-field asymmetric waveform ion mobility spectrometry: A new tool for mass spectrometry. *J. Chromatogr. A* **1058**, 3–19 (2004).

94. da Veiga Leprevost, F. *et al.* Philosopher: a versatile toolkit for shotgun proteomics data analysis. *Nat. Methods* **17**, 869–870 (2020).

95. Schweppe, D. K. *et al.* Characterization and Optimization of Multiplexed Quantitative Analyses Using High-Field Asymmetric-Waveform Ion Mobility Mass Spectrometry. *Anal. Chem.* **91**, 4010–4016 (2019).

96. Fang, P. *et al.* Evaluation and Optimization of High-Field Asymmetric Waveform Ion-Mobility Spectrometry for Multiplexed Quantitative Site-Specific N -Glycoproteomics. *Anal. Chem.* **93**, 8846–8855 (2021).

97. Ting, L., Rad, R., Gygi, S. P. & Haas, W. MS3 eliminates ratio distortion in isobaric multiplexed quantitative proteomics. *Nat. Methods* **8**, 937–940 (2011).

98. McAlister, G. C. *et al.* MultiNotch MS3 enables accurate, sensitive, and multiplexed detection of differential expression across cancer cell line proteomes. *Anal. Chem.* **86**, 7150–7158 (2014).

99. Fu, Q. *et al.* Comparison of MS2, synchronous precursor selection MS3, and real-time search MS3 methodologies for lung proteomes of hydrogen sulfide treated swine. *Anal.*

https://doi.org/10.26434/chemrxiv-2023-0szhj **ORCID:** https://orcid.org/0000-0001-8541-1404 Content not peer-reviewed by ChemRxiv. **License:** CC BY-NC-ND 4.0

Bioanal. Chem. **413**, 419–429 (2021).

100. Park, J. *et al.* Evaluating Linear Ion Trap for MS3-Based Multiplexed Single-Cell Proteomics. *Anal. Chem.* **95**, 1888–1898 (2023).

101. Schweppe, D. K. *et al.* Full-Featured, Real-Time Database Searching Platform Enables Fast and Accurate Multiplexed Quantitative Proteomics. *J. Proteome Res.* **19**, 2026–2034 (2020).

102. Boatner, L. M., Palafox, M. F., Schweppe, D. K. & Backus, K. M. CysDB: a human cysteine database based on experimental quantitative chemoproteomics. *Cell Chem. Biol.* **30**, 683-698.e3 (2023).

103. Yang, F., Jia, G., Guo, J., Liu, Y. & Wang, C. Quantitative Chemoproteomic Profiling with Data-Independent Acquisition-Based Mass Spectrometry. *J. Am. Chem. Soc.* **144**, 901–911 (2022).

104. Tsuboi, K. *et al.* Potent and Selective Inhibitors of Glutathione S -Transferase Omega 1 That Impair Cancer Drug Resistance. *J. Am. Chem. Soc.* **133**, 16605–16616 (2011).

105. Darabedian, N. *et al.* Depletion of creatine phosphagen energetics with a covalent creatine kinase inhibitor. *Nat. Chem. Biol.* **19**, 815–824 (2023).

106. Dubiella, C. *et al.* Sulfopin is a covalent inhibitor of Pin1 that blocks Myc-driven tumors in vivo. *Nat. Chem. Biol.* **17**, 954–963 (2021).

107. Pinch, B. J. *et al.* Identification of a potent and selective covalent Pin1 inhibitor. *Nat. Chem. Biol.* **16**, 979–987 (2020).

108. de Almeida, M. *et al.* AKIRIN2 controls the nuclear import of proteasomes in vertebrates. *Nature* **599**, 491–496 (2021).

109. Yang, J., Tallman, K. A., Porter, N. A. & Liebler, D. C. Quantitative Chemoproteomics for Site-Specific Analysis of Protein Alkylation by 4-Hydroxy-2-Nonenal in Cells. *Anal. Chem.* **87**, 2535–2541 (2015).

110. Murray, C. I., Uhrigshardt, H., O'Meally, R. N., Cole, R. N. & Van Eyk, J. E. Identification

https://doi.org/10.26434/chemrxiv-2023-0szhj **ORCID:** https://orcid.org/0000-0001-8541-1404 Content not peer-reviewed by ChemRxiv. **License:** CC BY-NC-ND 4.0

and quantification of S-nitrosylation by cysteine reactive tandem mass tag switch assay. *Mol. Cell. Proteomics* **11**, M111.013441 (2012).

111. Chanda, P. K. *et al.* Nuclear S-nitrosylation defines an optimal zone for inducing pluripotency. *Circulation* **140**, 1081–1099 (2019).

112. Li, Z., Liu, K., Xu, P. & Yang, J. Benchmarking Cleavable Biotin Tags for Peptide-Centric Chemoproteomics. *J. Proteome Res.* **21**, 1349–1358 (2022).

113. Jia, S., He, D. & Chang, C. J. Bioinspired Thiophosphorodichloridate Reagents for Chemoselective Histidine Bioconjugation. *J. Am. Chem. Soc.* **141**, 7294–7301 (2019).

114. Li, J. *et al.* ACR-Based Probe for the Quantitative Profiling of Histidine Reactivity in the Human Proteome. *J. Am. Chem. Soc.* **145**, 5252–5260 (2023).

115. Seki, Y. *et al.* Transition Metal-Free Tryptophan-Selective Bioconjugation of Proteins. *J. Am. Chem. Soc.* **138**, 10798–10801 (2016).

116. Herner, A. *et al.* 2-Aryl-5-carboxytetrazole as a New Photoaffinity Label for Drug Target Identification. *J. Am. Chem. Soc.* **138**, 14609–14615 (2016).

117. Allihn, P. W. A., Hackl, M. W., Ludwig, C., Hacker, S. M. & Sieber, S. A. A tailored phosphoaspartate probe unravels CprR as a response regulator in Pseudomonas aeruginosa interkingdom signaling. *Chem. Sci.* **12**, 4763–4770 (2021).

118. Chang, J. W., Montgomery, J. E., Lee, G. & Moellering, R. E. Chemoproteomic Profiling of Phosphoaspartate Modifications in Prokaryotes. *Angew. Chemie Int. Ed.* **57**, 15712–15716 (2018).

119. Conway, L. P. *et al.* Evaluation of fully-functionalized diazirine tags for chemical proteomic applications. *Chem. Sci.* **12**, 7839–7847 (2021).

https://doi.org/10.26434/chemrxiv-2023-0szhj **ORCID:** https://orcid.org/0000-0001-8541-1404 Content not peer-reviewed by ChemRxiv. **License:** CC BY-NC-ND 4.0